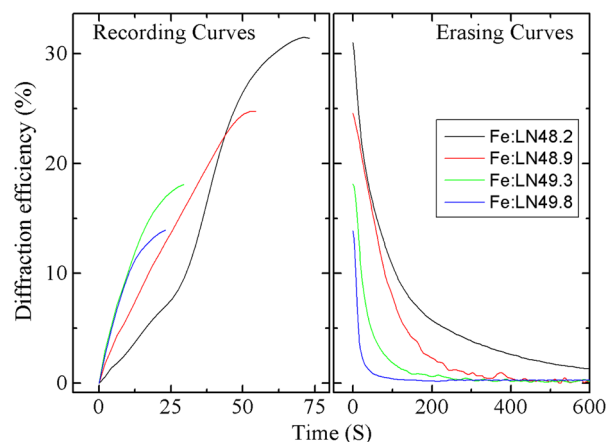


Photorefractive Properties Varied With Li Composition in $\text{LiNbO}_3:\text{Fe}$ Crystals

Volume 4, Number 5, October 2012

Xunan Shen
Wenbo Yan
Lihong Shi
Yongtao Wang
Fangfang Jia
Huibin Qiao
Guifeng Chen
Hongjian Chen
Aidiao Lin



DOI: 10.1109/JPHOT.2012.2219041
1943-0655/\$31.00 ©2012 IEEE

Photorefractive Properties Varied With Li Composition in LiNbO₃:Fe Crystals

Xunan Shen,^{1,3} Wenbo Yan,¹ Lihong Shi,² Yongtao Wang,¹ Fangfang Jia,¹
Huibin Qiao,¹ Guifeng Chen,¹ Hongjian Chen,¹ and Aidiao Lin¹

¹School of Material Science and Engineering, Hebei University of Technology, Tianjin 300130, China,

²Department of Physics, Tianjin Urban Construction Institute, Tianjin 300384, China

³Tianjin Power Source Institute, Tianjin 300384, China

DOI: 10.1109/JPHOT.2012.2219041
1943-0655/\$31.00 ©2012 IEEE

Manuscript received August 4, 2012; revised September 11, 2012; accepted September 11, 2012. Date of current version September 27, 2012. This work is supported in part by the National Natural Science Foundation under Grant 61108060, by the Excellent Young Researcher Foundation from Hebei University of Technology under Grant 2011001, and by the Key Project of Chinese Ministry of Education in 2012. Corresponding author: W. Yan (e-mail: Yanwenbo@hebut.edu.cn).

Abstract: LiNbO₃ : Fe crystals with different Li compositions were prepared in this paper. Both holographic storage and photo-induced light scattering experiments were carried out on these crystals. Our results showed that, with the increase of the Li composition in LiNbO₃ : Fe, the response time of the material was shortened largely, while the photo-induced light scattering in the crystals was suppressed significantly. These improvements of the photorefractive properties of LiNbO₃ : Fe were attributed to the change of polaronic system in the material. In addition, the rapid change of the photo-induced light scattering with the Li composition was found between 48.9 and 49.3 mol%. It was explained by the threshold effect of photo-induced light scattering with respect to the photovoltaic field.

Index Terms: Holography, oxide materials.

1. Introduction

Photorefractive materials can be utilized in data storage application, and several holographic storage demonstrators using lithium niobate (LiNbO₃) were presented in the last few decades [1]. As-grown pure LiNbO₃ crystal usually shows weak photorefractive effect, and it is unsuitable for practical use. Only after thermal reduction or at high light intensity pure LiNbO₃ can gain sufficient photorefractivity for data storage applications [2]. By contrast, as-grown Fe-doped LiNbO₃ (LiNbO₃ : Fe) crystal shows an enhanced photorefractivity even at low intensity. However, LiNbO₃ : Fe crystal still has two shortcomings: long response time and serious photo-induced light scattering [3], [4], which limit the further usage of this material in the data storage application.

Generally, the photorefractivity of LiNbO₃ has a close connection with the defects inside the crystal. Iyi *et al.* reported that, in the Li-deficient congruent crystal (CLN) with Li composition ($x_c = [\text{Li}]/([\text{Li}] + [\text{Nb}])$) around 48.3 mol%, there are a few percent of intrinsic defects such as Li vacancies and Nb antisite defects [5]. These defects may play the role of traps during the charge transport process and slow down the photorefractive response. Therefore, the high Li composition of near-stoichiometric LiNbO₃ (SLN), typically larger than 49.5 mol%, is expected to reduce the concentration of these intrinsic defects and markedly improves the photorefractive properties of pure LiNbO₃ [6], [7]. Moreover, Malovichko *et al.* and Kostitskii *et al.* investigated the composition dependence of optical properties of pure SLN and found the correlation of the intrinsic defects to Raman lines, dispersion of birefringence, photorefractivity, and polaron luminescence [8]–[10].

TABLE 1

Measured parameters of the samples

Sample	[Li] (mol%)	α_0 (cm ⁻¹)	[Fe ²⁺](10 ²⁴ /m ³)	[Fe ²⁺]/[Fe ³⁺]	τ_r (s)	τ_e (s)	η_0 (%)	M/#	R ₀
Fe:LN _{48,2}	48.2±0.05	4.52±0.03	1.17±0.01	0.155±0.001	33.6±0.1	277.2±0.1	31±1	4.6±0.1	0.47±0.02
Fe:LN _{48,9}	48.9±0.05	2.65±0.03	0.69±0.01	0.085±0.001	16.8±0.1	168.7±0.1	25±1	5.0±0.2	0.42±0.02
Fe:LN _{49,3}	49.3±0.05	2.09±0.03	0.54±0.01	0.066±0.001	6.3±0.1	83.4±0.1	18±1	5.6±0.3	0.12±0.02
Fe:LN _{49,8}	49.8±0.05	0.85±0.03	0.22±0.01	0.026±0.001	4.9±0.1	26.6±0.1	14±1	2.0±0.2	0±0.02

Similarly, in case of LiNbO₃ doped with Fe, the elevation of Li composition also has such improving effect. Kitamura and Furukawa *et al.* studied near-stoichiometric Fe-doped LiNbO₃ and found that the intrinsic defect control of photorefractive crystals is of key importance for the enhancement of photorefractive parameters of LiNbO₃ : Fe [11]–[14]. Hatano *et al.* then studied the influence of the dual oxidation states (Fe²⁺ and Fe³⁺) on the photorefractive properties of the near-stoichiometric LiNbO₃ : Fe and established some relationship between the photorefractive parameters and the absorption coefficient of the material [13]. Li *et al.* grown a series of Fe-doped SLN with different doping levels and found that a high doping concentration would destroy the stoichiometric structure of the crystals [15]. Despite the detailed studies on the congruent and near-stoichiometric LiNbO₃ : Fe separately [11]–[15], no result was published on LiNbO₃ : Fe with the compositions between congruent and stoichiometric points, which is unfavorable to the tailor of the photorefractive properties of LiNbO₃ : Fe through modifying the Li composition.

The photo-induced light scattering is another problem that one has to overcome for the data storage. One way to solve this problem is to optimize the crystal through codoping with optical-damage-resistant dopants. It was reported that, when LiNbO₃ : Fe was codoped with the elements such as Mg and Zn, the photo-induced light scattering can be suppressed to some extent [16], [17]. However, for these dopants, there is a so-called “threshold concentration,” above which the diffraction efficiency of the crystal decreases apparently and a huge percentage (about 80% in Mg-doped LiNbO₃ : Fe) of the diffraction efficiency is sacrificed for the codoping [18]. Furthermore, too much doping may induce the stripe in the crystal and make the growth of the highly optical homogeneous crystal difficult [19]. Elevating Li composition is another important way to optimize the crystal and it is likely to suppress the photo-induced light scattering sufficiently. But regarding the behavior of the photo-induced light scattering when the Li composition of LiNbO₃ : Fe is modified, no investigation was reported till now. In this paper, Fe-doped LiNbO₃ crystals with different Li compositions are prepared. The photorefractive parameters such as diffraction efficiency, response time, and dynamic range coefficient, as well as the photo-induced light scattering behavior of these LiNbO₃ : Fe crystals are systematically studied.

2. Experimental Details

The starting congruent LiNbO₃ : Fe crystal was grown along c-axis through Czochralski method. In order to obtain a single crystal with uniform domain, the postgrowth poling was performed around the Curie temperature within the air atmosphere. This procedure can also guarantee the whole crystal in a uniform oxidation state. Four rectangle plates (10 × 5 × 1 mm³) were cut from the same region of the boule in order to make sure all plates have identical Fe concentrations. Then, the Li compositions of these plates were modified to different values through vapor-transport-equilibration (VTE) method [20]. All of the samples were optically polished Y-cut sheets with 1-mm thickness. The Li compositions of these samples were characterized by the measurement of the Raman linewidth, which allows the determination of the Li composition within an absolute accuracy of 0.1% [21]. In our experiments, the E-mode at 153 cm⁻¹ was chosen, and the linewidths of the samples were measured to be 10.19, 8.71, 7.87, and 6.82 cm⁻¹, respectively. Through the well-known linear relationship between Li composition and the line width Γ ($x_c = 53.03 - 0.4739\Gamma$), the Li compositions of the samples can be estimated (see Table 1). The absorption spectra of the samples were measured through shimadzu UV-365 spectrometer. As shown in Fig. 1, these

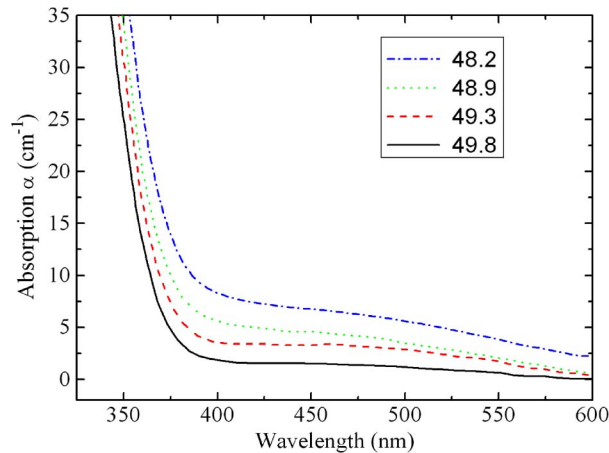


Fig. 1. Absorption spectra of the samples with different compositions.

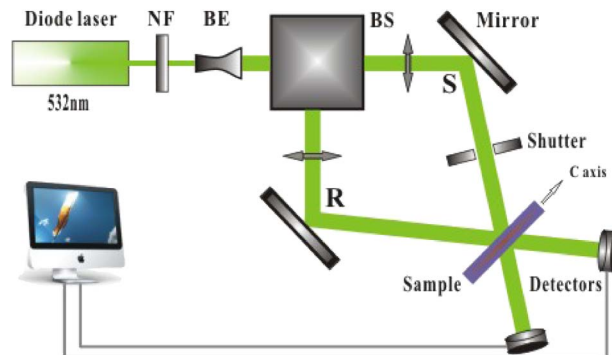


Fig. 2. Holographic experimental setup. NF: Neutral Filter; BE: Beam Expander; BS: Beam Splitter.

samples have different absorption curves, indicating that their starting oxidation states have been modified to different extent, depending on the Li-rich atmosphere used in their VTE procedures. The concentration of filled iron traps $[\text{Fe}^{2+}]$ can be deduced from the absorption coefficient α_0 at the wavelength of 532 nm [22]. If we consider the distribution coefficient of Fe simply as one [23], the total iron concentration $[\text{Fe}]$ in the crystal can be estimated as $8.74 \times 10^{24} \text{ m}^{-3}$ for the doping level of 0.025 wt.% in our case. Thus, the concentration of empty traps $[\text{Fe}^{3+}]$ can be calculated through $[\text{Fe}] - [\text{Fe}^{2+}]$ (see Table 1).

The photorefractive properties of the samples were firstly studied through holographic storage experiment at room temperature. Fig. 2 shows the basic setup of this experiment. The holographic grating was written by two expanded e-polarized beams ($I_S = I_R = 1.75 \times 10^3 \text{ W/m}^2$, the expanded beam diameter is about 6 mm, and the crossing angle of the two beams is 36° in air) with the grating wave vector aligned along the c-axis. The two surfaces perpendicular to the c-axis were short circuited to prevent space-charge accumulation. For each sample, we recorded the temporal curve of diffraction efficiency, which is defined as the ratio between the intensities of the diffracting light and of the transmitting light without grating, by blocking the signal beam (denoted as “S” in Fig. 2) from time to time. After the diffraction efficiency had reached the saturation, the signal beam was blocked completely, and the sample was homogeneously illuminated by the single reference beam (denoted as “R” in Fig. 2) for grating erasure. Hereafter, η_0 represents the saturation diffraction efficiency, and the recording time τ_r (or erasing time τ_e) is defined as the period of time taken to reach $(1 - 1/e)$ (or $1/e$) of the saturation grating strength A_0 . Note that the grating strength A is

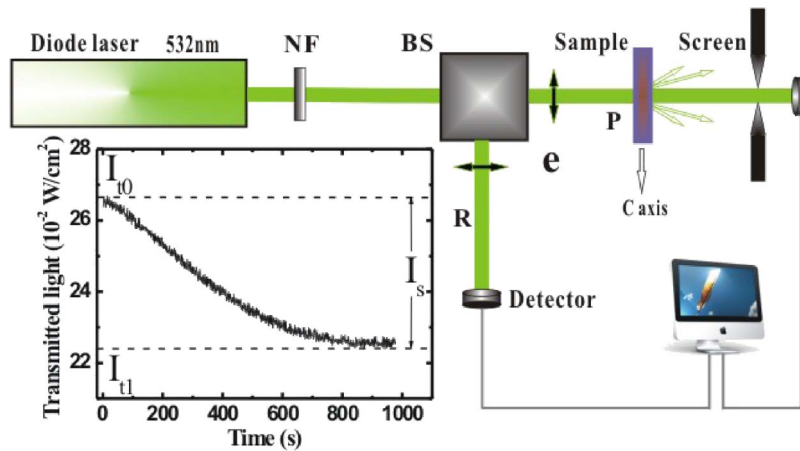


Fig. 3. Experimental setup for measuring the photo-induced light scattering. NF: Neutral Filter; BS: Beam Splitter.

proportional to the square root of the diffraction efficiency ($\sqrt{\eta}$). Generally, the erasing time τ_e reflects the decay speed of the grating under uniform illumination, and this process is mainly governed by the photoconductivity of the sample. Therefore, the photoconductivity σ can be obtained directly from the erasing time τ_e through the relationship $\sigma = \epsilon\epsilon_0/\tau_e$. By contrary, the recording time τ_r characterizes the establishing speed of the grating under the interference fringes, and it is not only related to the photoconductivity but also has a close connection with the complicated dynamic process of the grating establishment. Nevertheless, the recording time still can be used as an indicator of the sample photoconductivity.

The setup for measuring the photo-induced light scattering is shown in Fig. 3, where the pump beam “P”, with a diameter of 2 mm, impinges the sample along the y -axis. The light intensity was varied using a neutral density filter, and a screen was used to block the scattering light. The transmitted pump light was collected by a detector, and the reference light “R” was used to reduce the drifts caused by laser power fluctuation. Typical curve of the transmitted light is shown in the inset. With the buildup of the photo-induced light scattering, the transmitted light will gradually lose its energy and finally saturates at a certain intensity level. The time for the transmitted intensity to reach the saturation may vary from several seconds to some minutes, depending on the pump intensity and the Li composition of the sample. From the temporal curve of the transmitted light, we can calculate the photo-induced light scattering light intensity $I_S (= I_{t0} - I_{t1})$, and the photo-induced light scattering can be characterized by an unified value $R (= I_S/I_{t0})$.

3. Results

As mentioned in the experimental section, all samples have the same starting oxidation state, and during the VTE procedure, they experienced the similar heat-treatment histories apart from the different Li-rich atmosphere used. However, as listed in Table 1, the samples show different absorption spectra: α_0 decreases with the increase of the Li composition. This result means that Li incorporation may induce additional oxidization effect to CLN:Fe crystal. The recording and erasing curves of the samples with different compositions are shown in Fig. 4. τ_r , τ_e , and η_0 are obtained from this figure and listed in Table 1. It can be seen that both η_0 and response time (including τ_r and τ_e) decrease with the increase of Li composition. When the Li composition comes to 49.8 mol%, τ_r and τ_e are just 4.9 and 26.6 s, which are several times shorter than that of the congruent one. Hatano *et al.* reported that the photorefractive properties of the near-stoichiometric $\text{LiNbO}_3 : \text{Fe}$ are highly dependent on the absorption coefficient of the material. For example, the response time show an increase with the decrease of the absorption [13]. But in our case, the response time decreases in spite of the decreasing absorption, which indicates that the Li composition have a

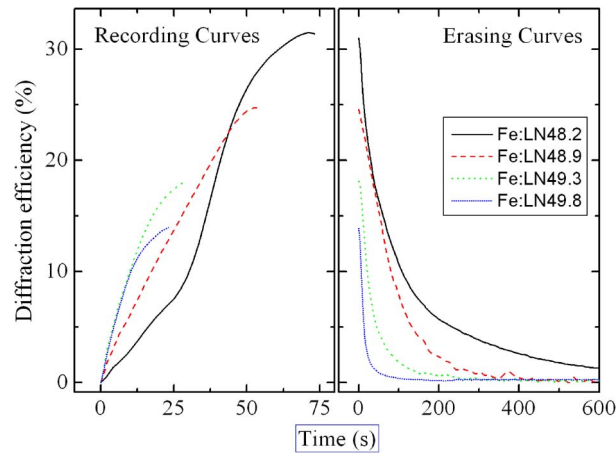


Fig. 4. The recording and erasing curves of the samples with different compositions.

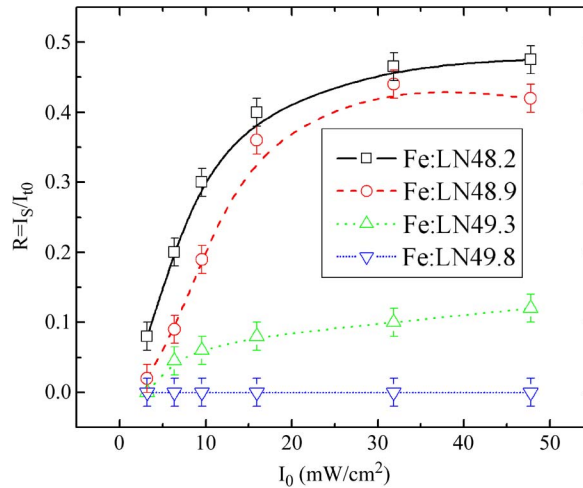


Fig. 5. Unified photo-induced light scattering value (R) plotted versus pump light intensity (I_0).

dominating effect on the photorefractive properties as compared with the absorption of the crystal. The large decrease of the response time means elevating Li composition can enhance significantly the photoconductivity of the crystal, and it is certainly helpful to accelerate the recording and erasing of hologram in this material. Dynamic range coefficient ($M/\#$) is another important parameter in holographic application. In general, $M/\#$ is defined as $A_0\tau_e/\tau_r$ [24], and thus, it is proportional to the product of the square root of η_0 and the ratio of τ_e and τ_r . As listed in Table 1, $M/\#$ increases slightly from the congruent point to the intermediate composition of 49.3. The low $M/\#$ value for the most near-stoichiometric sample reveals that too much higher composition is not helpful to recording multiple holograms.

The change of scattered light intensity value (R) with the pump light intensity is shown in Fig. 5. It is clear that, for any sample, R value gradually goes up with pump light intensity (I_0) and reaches a saturated value (R_0) at relative high pump intensity. Moreover, R_0 decreases significantly with the increase of the Li composition. Especially when the Li composition reaches 49.8 mol%, R_0 value tends to zero, which means the light-scattering phenomenon disappears completely. It should be noted that a huge percentage (about 80%) of diffraction efficiency is sacrificed to suppress the photo-induced light scattering in highly Mg-doped $\text{LiNbO}_3 : \text{Fe}$ [16]. But for $\text{Fe} : \text{LN}_{49.8}$, the tradeoff (about 50%) of diffraction efficiency for the complete suppression of photo-induced light scattering

is relatively less, indicating that elevating the Li composition could be a better way for the balance between the different photorefractive parameters of $\text{LiNbO}_3 : \text{Fe}$.

In general, the photoconductivity can be described by the relationship $\sigma \propto e\mu[\text{Fe}^{2+}]/[\text{Fe}^{3+}]\tau$, where e is a constant representing the electron charge, and μ and τ , which are often considered as parameters with fixed values, are the mobility and the lifetime of charge transport species, respectively [25]. Our data regarding the response time reveal that the photoconductivity increases with the increase of the Li composition of $\text{LiNbO}_3 : \text{Fe}$. However, the absorption measurement shows that the ratio $[\text{Fe}^{2+}]/[\text{Fe}^{3+}]$ decreases with the increase of the Li composition. Since the electron charge is constant undoubtedly, we have to pay attention to the other two parameters μ and τ , which may be influenced by the Li composition and contribute to the composition dependence of the photoconductivity. Recently, Schirmer *et al.* published a comprehensive paper regarding the bulk photovoltaic effect of $\text{LiNbO}_3 : \text{Fe}$ and its polaron-based microscopic interpretation [26]. They pointed out that the free conduction polarons $(\text{Nb}_{\text{Nb}})^{4+}$ contribute a lot to the photoconductivity during their lifetime τ , i.e., as long as they are not trapped by the deep defects. It is well known that the antisite niobium ions $(\text{Nb}_{\text{Li}})^{5+}$, a kind of deep defects in LN, may trap the electron of the free polarons. This trapping certainly leads to the decrease of the product of μ and τ of the free polarons. Since the concentration of the antisite niobium ions gradually decreases with the increase of the Li composition, we found the significantly increased photoconductivity in Fe-doped SLN.

The above viewpoint could also partly explain the result that photo-induced light scattering is suppressed sufficiently in $\text{LiNbO}_3 : \text{Fe}$ with high Li composition. In general, photovoltaic field (E_{ph}) can be described by bulk photovoltaic currents (j_{ph}) and photoconductivity (σ_{ph}) as $E_{\text{ph}} = j_{\text{ph}}/\sigma_{\text{ph}} \propto [\text{Fe}^{3+}]/\mu\tau$, if the dark conductivity is far smaller than the photoconductivity [25]. Since the variations of $[\text{Fe}^{3+}]$ in all samples are not so large (smaller than 15%), we consider E_{ph} dominated by the ratio $1/\mu\tau$. Thus, the photovoltaic field produced in $\text{LiNbO}_3 : \text{Fe}$ should decrease with the increase of the Li composition. As a result, the photo-induced light scattering in Fe-doped SLN is nearly absent.

Another noticeable result regarding the photo-induced light scattering is the rapid change of R when the Li composition is increasing from 48.9 to 49.3 mol%. In fact, such kind of sharp change of the properties within some special composition range has already been reported in pure LN. Hesselink *et al.* reported that the two-photon sensitivity of pure LN shows an abrupt increase within the range from 49.5 to 49.6 mol%, and they attributed it to the sudden hardening of the crystal lattice due to the decreased density of $\text{Nb}_{\text{Li}}^{4+}$ defects [27]. Abdi *et al.* reported an abrupt slope change for both EO coefficients within the range from 49.0 to 49.2 mol%, and they attributed it to the dramatic variation of the intrinsic defect system [28]. Kostrikskii *et al.* observed the similar nonmonotonous composition dependences of light-induced refractive index change, photorefractive sensitivity, and normalized polaron luminescence, and they tried to explain these peculiarities by the distance-dependent excitation and recombination rates of polarons [8], [9]. Since nominally pure LN always has traces of iron, the above explanations may also be valid for the composition dependence of R value in Fe-doped LN. However, it should be noted that Fe-doped LN usually has much stronger photorefractivity than pure LN at low intensity, and its strong photorefractivity may lead to many complicated optical phenomena. Therefore, the rapid change of R in our paper can also be attributed to another origin: the threshold effect of photo-induced light scattering with respect to the photovoltaic field [29]. This effect was firstly reported by Zhang *et al.* for Fe-doped LN, and it was found that when the photovoltaic field is decreased below a threshold value, the photo-induced light scattering will be suppressed greatly [29]. Therefore, the rapid change of R in our case could be explained by the fact that, when the Li composition is increasing from 48.9 to 49.3 mol%, the photovoltaic field produced in $\text{LiNbO}_3 : \text{Fe}$ decreases sufficiently and already situates below the threshold value at which the photo-induced light scattering is suppressed greatly.

The origin of the threshold effect of photo-induced light scattering is related to the particular nature (multithree-wave mixing) of the fanning noise amplification in $\text{LiNbO}_3 : \text{Fe}$ [30]. In fact, other novel mechanism of fanning noise amplification was also proposed for the photorefractive materials. Goulkov *et al.* suggested the fanning noise amplification as a normal two-wave mixing

process but taking into account the nonzero shift in the temporal frequency of the scattered light, the competition of photovoltaic and diffusion, and the contribution of nonthermalized electrons in the diffusion space-charge transport [31]. They showed that this model can explain qualitatively all features of the photoinduced scattering measured in $\text{LiTaO}_3 : \text{Fe}$ crystals and lately applied this model to nominally pure LiNbO_3 successfully [32]. Now, we are trying to explain our results under this fanning mechanism, and the study is still underway.

Our above discussion is based on the fact that the dark conductivity is neglectable. However, if the dark conductivity is comparable to the photoconductivity, other interpretation must be considered for our results. For example, high dark conductivity can induce the limitation of the space-charge field and, in turn, leads to the decrease of the diffraction efficiency and the suppression of the photo-induced light scattering. It is well known that LN:Fe crystal is very sensitive to green illumination, but it has a long dark-storage lifetime at room temperature. It means that the dark conductivity of LN:Fe normally is quite small as compared with the photoconductivity produced by the light intensities (several to tens of mW/cm^2) in our experiments. Certainly, despite thermal reduction, the dark conductivity of LN:Fe can be elevated to a high level and contributes to the suppression of the photorefraction [33]. However, all samples in our case have oxidation starting states, and during the VTE procedure, their oxidation extents are further enhanced. Although the Li incorporation may lead to some increase of the dark conductivity, the dark conductivity still cannot be comparable with the greatly enhanced photoconductivity in LN:Fe crystals.

As a matter of fact, the thermal reduction usually gives rise to the formation of large amount of bipolarons in CLN crystals [8], [9]. These polarons can contribute to the visible absorption (overlapped with the absorption induced by Fe^{2+}), increase the dark conductivity of the crystal, and therefore play important roles in the photorefractive process. Since our samples are all in oxidation state, the density of bipolarons could be considered as in low level and their roles may be neglected in comparison with the significant photorefractive effect of Fe^{2+} . For detailed investigations of the bipolarons in our samples, many other experiments such as EPR and pump-probe absorption measurement are needed.

4. Conclusion

In summary, Fe-doped LiNbO_3 crystals with different Li compositions were prepared and studied in this paper. It was found that, with the increase of the Li composition in $\text{LiNbO}_3 : \text{Fe}$, the response time was shortened largely while the photo-induced light scattering was suppressed significantly. The effect of Li incorporation on the charge transport was suggested to account for these improvements.

Acknowledgment

The author would like to thank the reviewers for their valuable comments, as well as Prof. Y. Kong and Dr. X. Li for sample preparation and basic characterization.

References

- [1] P. Günter and J. P. Huignard, *Photorefractive Materials and Their Applications*. Heidelberg, Germany: Springer-Verlag, 1989.
- [2] W. Yan, P. Minzioni, G. Nava, P. Galinetto, L. Shi, and V. Degiorgio, "Critical composition of reduced pure- LiNbO_3 crystals: A sudden change in optical properties," *Appl. Phys. Lett.*, vol. 98, no. 15, pp. 151112-1–151112-3, Apr. 2011.
- [3] S. Li, S. Liu, Y. Kong, J. Xu, and G. Zhang, "Enhanced photorefractive properties of $\text{LiNbO}_3 : \text{Fe}$ crystals by HfO_2 codoping," *Appl. Phys. Lett.*, vol. 89, no. 10, pp. 101126-1–101126-3, Sep. 2006.
- [4] F. Liu, Y. Kong, X. Ge, H. Liu, S. Liu, S. Chen, R. Rupp, and J. Xu, "Improved sensitivity of nonvolatile holographic storage in triply doped $\text{LiNbO}_3 : \text{Zr, Cu, Ce}$," *Opt. Expr.*, vol. 18, no. 6, pp. 6333–6339, Mar. 2010.
- [5] N. Iyi, K. Kitamura, Y. Yajima, and S. Kimura, "Defect structure model of MgO-doped LiNbO_3 ," *J. Solid State Chem.*, vol. 118, no. 1, pp. 148–152, Aug. 1995.
- [6] X. Chen, D. Zhu, B. Li, T. Ling, and Z. Wu, "Fast photorefractive response in strongly reduced near-stoichiometric LiNbO_3 crystals," *Opt. Lett.*, vol. 26, no. 13, pp. 998–1000, Jul. 2001.

- [7] X. Chen, B. Li, J. Xu, D. Zhu, S. Pan, and Z. Wu, "LiNbO₃ grown from congruent melts containing K₂O," *J. Appl. Phys.*, vol. 90, no. 3, pp. 1516–1520, Aug. 2001.
- [8] S. M. Kostritskii and O. G. Sevostyanov, "Composition dependence of photorefractive effect in nominally pure LiNbO₃ crystals," *Radiat. Effects Defects Solids*, vol. 150, no. 1, pp. 315–320, Sep. 1999.
- [9] S. M. Kostritskii, O. G. Sevostyanov, P. Bourson, M. Aillerie, M. D. Fontana, and D. Kip, "Comparative study of composition dependences of photorefractive and related effects in LiNbO₃ and LiTaO₃ crystals," *Ferroelectrics*, vol. 352, no. 2, pp. 61–71, Jun. 2007.
- [10] G. I. Malovichko, V. G. Grachev, E. P. Kokanyan, O. F. Schirmer, K. Betzler, B. Gather, F. Jermann, S. Klauer, U. Schlarb, and M. Wöhlecke, "Characterization of stoichiometric lithium niobate grown from melts containing K₂O," *J. Appl. Phys.*, vol. A56, no. 2, pp. 103–108, Sep. 1993.
- [11] K. Kitamura, Y. Furukawa, Y. Ji, M. Zgonik, C. Medrano, G. Montemezzani, and P. Günter, "Photorefractive effect in LiNbO₃ crystals enhanced by stoichiometry control," *J. Appl. Phys.*, vol. 82, no. 3, pp. 1006–1009, Aug. 1997.
- [12] Y. Furukawa, K. Kitamura, Y. Ji, G. Montemezzani, M. Zgonik, C. Medrano, and P. Günter, "Photorefractive properties of iron-doped stoichiometric lithium niobate," *Opt. Lett.*, vol. 22, no. 8, pp. 501–503, Apr. 1997.
- [13] H. Hatano, T. Yamaji, S. Tanaka, Y. Furukawa, and K. Kitamura, "Investigation of the oxidation state of Fe in stoichiometric Fe : LiNbO₃ for digital holographic recording," *Jpn. J. Appl. Phys.*, vol. 38, no. 3B, pp. 1820–1825, Mar. 1999.
- [14] H. Liu, X. Xie, Y. Kong, W. Yan, X. Li, L. Shi, J. Xu, and G. Zhang, "Photorefractive properties of near-stoichiometric lithium niobate crystals doped with iron," *Opt. Mater.*, vol. 28, no. 3, pp. 212–215, Feb. 2006.
- [15] H. Li, Y. Fan, F. Guo, Y. Xu, and L. Zhao, "Growth and spectroscopic characterization of Fe₂O₃ highly doped near-stoichiometric LiNbO₃ single crystals," *J. Cryst. Growth*, vol. 303, no. 2, pp. 651–654, May 2007.
- [16] T. Volk, N. Rubiniina, and M. Wöhlecke, "Optical-damage-resistant impurities in lithium niobate," *J. Opt. Soc. Amer. B, Opt. Phys.*, vol. 11, no. 9, pp. 1681–1687, Sep. 1994.
- [17] M. Simon, F. Jermann, T. Volk, and E. Krätzig, "Influence of zinc doping on the photorefractive properties of lithium niobate," *Phys. Stat. Sol. (A)*, vol. 149, no. 2, pp. 723–732, Jun. 1995.
- [18] G. Zhang, J. Xu, S. Liu, Q. Sun, G. Zhang, Q. Fang, and C. Ma, "Study of resistance against photorefractive photo-induced light scattering in LiNbO₃:Fe,Mg crystals," *Proc. SPIE*, vol. 2529, p. 14, Nov. 1995.
- [19] L. Wang, S. Liu, Y. Kong, S. Chen, Z. Huang, L. Wu, R. Rupp, and J. Xu, "Increased optical-damage resistance in tin-doped lithium niobate," *Opt. Lett.*, vol. 35, no. 6, pp. 883–885, Mar. 2010.
- [20] D. H. Jundt, M. M. Fejer, and R. L. Byer, "Optical properties of lithium-rich lithium niobate fabricated by vapor transport equilibration," *J. Quantum Electron.*, vol. 26, no. 1, pp. 135–138, Jan. 1990.
- [21] M. Wöhlecke, G. Corradi, and K. Betzler, "Optical methods to characterise the composition and homogeneity of lithium niobate single crystals," *Appl. Phys. B*, vol. 63, no. 4, pp. 323–330, Oct. 1996.
- [22] H. Kurz, E. Krätzig, W. Keune, H. Engelmann, U. Gonser, B. Dischler, and A. Räuber, "Photorefractive centers in LiNbO₃, studied by optical-, Mössbauer- and EPR-methods," *J. Appl. Phys.*, vol. 12, no. 4, pp. 355–368, Apr. 1977.
- [23] K. Peithmann, A. Wiebrock, and K. Buse, "Photorefractive properties of highly-doped lithiumniobate crystals in the visible and near-infrared," *Appl. Phys. B*, vol. 68, no. 5, pp. 777–784, May 1999.
- [24] F. H. Mok, G. W. Burr, and D. Psaltis, "System metric for holographic memory systems," *Opt. Lett.*, vol. 21, no. 12, pp. 896–898, Jun. 1996.
- [25] K. Buse, "Light-induced charge transport processes in photorefractive crystals I: Models and experimental methods," *Appl. Phys. B*, vol. 64, no. 3, pp. 273–291, Mar. 1997.
- [26] O. F. Schirmer, M. Imlau, and C. Merschjann, "Bulk photovoltaic effect of LiNbO₃: Fe and its small-polaron-based microscopic interpretation," *Phys. Rev. B*, vol. 83, no. 16, pp. 165106-1–165106-13, Apr. 2011.
- [27] L. Hesselink, S. Orlov, A. Liu, A. Akella, D. Lande, and R. Neurgaonkar, "Photorefractive materials for nonvolatile volume holographic data storage," *Science*, vol. 282, no. 5391, pp. 1089–1094, Nov. 1998.
- [28] F. Abdi, M. D. Fontana, M. Aillerie, and P. Bourson, "Coexistence of Li and Nb vacancies in the defect structure of pure LiNbO₃ and its relationship to optical properties," *Appl. Phys. A*, vol. 83, no. 3, pp. 427–434, Jun. 2006.
- [29] G. Zhang, G. Zhang, S. Liu, J. Xu, G. Tian, and Q. Sun, "Theoretical study of resistance against photo-induced light scattering in LiNbO₃ : M (M = Mg²⁺, Zn²⁺, In³⁺, Sc³⁺) crystals," *Opt. Lett.*, vol. 22, no. 22, pp. 1666–1668, Nov. 1997.
- [30] G. Zhang, G. Tian, S. Liu, J. Xu, G. Zhang, and Q. Sun, "Noise amplification mechanism in LiNbO₃ : Fe crystal sheets," *J. Opt. Soc. Amer. B*, vol. 14, no. 11, pp. 2823–2830, Nov. 1997.
- [31] M. Goukov, S. Odoulov, Th. Woike, J. Imbrock, M. Imlau, E. Krätzig, C. Bäumer, and H. Hesse, "Holographic light scattering in photorefractive crystals with local response," *Phys. Rev. B*, vol. 65, no. 19, pp. 195111-1–195111-6, May 2002.
- [32] M. Goukov, M. Imlau, and Th. Woike, "Photorefractive parameters of lithium niobate crystals from photoinduced light scattering," *Phys. Rev. B*, vol. 77, no. 23, pp. 235110-1–235110-7, Jun. 2008.
- [33] W. Yan, X. Shen, L. Shi, F. Jia, H. Qiao, H. Chen, G. Chen, Y. Lu, S. Zhang, and A. Lin, "Suppression of the photoinduced light scattering in LiNbO₃ : Fe by redox treatment and incoherent homogeneous illumination," *Appl. Phys. A*, vol. 108, no. 3, pp. 615–620, Sep. 2012.